Plant Cell Reports (2018) 37:727–739
https://doi.org/10.1007/s00299-018-2263-z

ORIGINAL ARTICLE

The superoxide dismutase genes might be required for appropriate development of the ovule after fertilization in *Xanthoceras sorbifolium*

Qingyuan Zhou[1] · **Qing Cai**[1]

Received: 18 December 2017 / Accepted: 24 January 2018 / Published online: 31 January 2018

Abstract

Key message **Superoxide dismutase genes were expressed differentially along with developmental stages of fertilized ovules in *Xanthoceras sorbifolium*, and the *XsMSD* gene silencing resulted in the arrest of fertilized ovule development.**

Abstract A very small percentage of mature fruits (ca. 5%) are produced relative to the number of bisexual flowers in *Xanthoceras sorbifolium* because seeds and fruits are aborted at early stages of development after pollination. Reactive oxygen species (ROS) in plants are implicated in an extensive range of biological processes, such as programmed cell death and senescence. Superoxide dismutase (SOD) activity might be required to regulate ROS homeostasis in the fertilized ovules of *X. sorbifolium*. The present study identified five *SOD* genes and one *SOD* copper chaperone gene in the tree. Their transcripts were differentially expressed along different stages of fertilized ovule development. These genes showed maximum expression in the ovules at 3 days after pollination (DAP), a time point in which free nuclear endosperm and nucleus tissues rapidly develop. The *XsCSD1, XsFSD1* and *XsMSD* contained seven, eight, and five introns, respectively. Analysis of the 5′-flanking region of *XsFSD1* and *XsMSD* revealed many *cis*-acting regulatory elements. Evaluation of *XsMSD* gene function based on virus-induced gene silencing (VIGS) indicated that the gene was closely related to early development of the fertilized ovules and fruits. This study suggested that *SOD* genes might be closely associated with the fate of ovule development (aborted or viable) after fertilization in *X. sorbifolium*.

Keywords *Xanthoceras sorbifolium* · Fertilized ovule development · Superoxide dismutase gene family · Expression

Introduction

Xanthoceras sorbifolium, a member of the family Sapindaceae, is a small- to medium-sized tree that grows up to 10 m in height and is endemic to north China. The seed of *X. sorbifolium* contains ca. 34% edible oil of high quality that can be used for various purposes including as feedstock for the production of biodiesel (Zhou and Liu 2012). The trees produce only a very small percentage of mature fruits (ca. 5%) relative to the number of bisexual flowers because seeds are aborted at the early stages of development after pollination, resulting in the abortion of young fruits and severely low seed yield (Zhou et al. 2017). To date, little is known about the cytological and molecular mechanisms of the abortion of fruits and fertilized ovules in *X. sorbifolium*.

Reactive oxygen species (ROS) are regarded as inevitable byproducts of normal cell metabolism and are continually generated in chloroplasts, mitochondria, peroxisomes, and glyoxysomes (Suzuki et al. 2012; Singh et al. 2016). ROS are highly reactive and toxic and can lead to the oxidative destruction of cell structures and molecules (Sandalio et al. 2013). However, potentially harmful ROS are also used as signaling molecules and have been implicated in an extensive range of biological processes such as biotic and abiotic stress responses, embryo sac development, senescence, programmed cell death, and hormonal and systematic signaling (Tsukagoshi et al. 2010; María et al. 2013; Singh et al. 2016). The dual role of ROS is mainly dependent on the ROS level and site of action. ROS fluctuations and homeostasis are regulated by a complex

Communicated by Qiaochun Wang.

Electronic supplementary material The online version of this article (https://doi.org/10.1007/s00299-018-2263-z) contains supplementary material, which is available to authorized users.

✉ Qingyuan Zhou
qyzhou@ibcas.ac.cn

[1] Key Laboratory of Plant Resources, Institute of Botany, Chinese Academy of Sciences, Beijing, China

network of ROS production and scavenging that operates in various subcellular compartments (Mittler et al. 2011; Gupta et al. 2017).

The superoxide dismutases (SODs; EC 1.15.1.1) are the first line of antioxidant enzyme defense systems against ROS and they catalyze the dismutation of superoxide anion (O_2^-) to molecular oxygen (O_2) and hydrogen peroxide (H_2O_2) (McCord and Fridovich 1988). Three different metal-containing SOD enzymes are found in plant tissues (Kliebenstein et al. 1998). These SODs are the products of different genes and they are classified by the redox metal cofactors in the active site into three families, namely copper–zinc SOD (CuZnSOD, CSD), manganese SOD (MnSOD, MSD) and iron SOD (FeSOD, FSD). Multiple SODs are present for the removal of O_2^- in various compartments of plant cells where O_2^- radicals are generated (Kliebenstein et al. 1998).

SOD isoenzyme activity might be required to regulate ROS homeostasis along different stages of development of fertilized ovules in *X. sorbifolium*. This regulation might be closely associated with the fate of ovule development (aborted or viable) in the plant. To test this hypothesis, we cytologically examined the development of *X. sorbifolium* ovules at various stages of post-fertilization and identified full-length cDNAs of *SOD* genes. The genomic sequences of *XsCSD1, XsFSD1* and *XsMSD* genes were isolated. To further understand the transcriptional regulatory role of *XsSOD* genes, *XsFSD1* and *XsMSD* 5′-flanking sequences were isolated by thermal asymmetric interlaced PCR (TAIL-PCR), and the *cis*-acting regulatory elements of *XsSOD* promoters were analyzed. We used quantitative real-time polymerase chain reaction (qRT-PCR) to analyze the pattern of expression of *SOD* genes during the development of fertilized ovules.

We tested the application of the Tobacco rattle virus (TRV)-based virus-induced gene silencing (VIGS) system in young fruits of *X. sorbifolium*. TRV-*XsMSD* constructs were capable of silencing *XsMSD* expression, resulting in the abortion of the young fruits and the ovules after pollination. These results indicated that the *XsMSD* gene might be required for appropriate development of the fertilized ovules in *X. sorbifolium*.

Materials and methods

Plant materials

Ten-year-old trees of *X. sorbifolium* were located in the Botanical Garden, Institute of Botany, Chinese Academy of Sciences. Bisexual flowers were hand cross-pollinated and ovules of different ages, from young ovule until mature seed, were sampled for various experimental purposes.

Cytological analysis of fertilized ovules

The sampled ovules were fixed with 2.5% glutaraldehyde in 0.05 M phosphate buffer (pH 7.2). The specimens were left in the fixative for 2–4 h at room temperature and then overnight at 4 °C. The material was dehydrated through a graded acetone series and embedded in Spurr's resin (Spurr 1969). Semithin sections (1 μm thick) were cut with a diamond knife on a Leica Ultracut R. The sections were stained with 0.5% toluidine blue O and observed with a light microscope.

Protein extraction and SOD activity assay

The fertilized ovules were ground with 150 mM of Tris–HCl (pH 7.2) and the homogenate was centrifuged at 18,000*g* at 4 °C for 15 min. Total protein (50 mg) was separated on a 10% nondenaturing polyacrylamide gel in Tris-Gly buffer (pH 8.3) and determined by Coomassie blue staining. The gel was incubated in 750 μM of nitroblue tetrazolium (NBT) solution for 15 min, rinsed with distilled water, and transferred to 100 mM of potassium phosphate buffer (pH 7.0) containing 0.028 mM of riboflavin and 28 mM of TEMED (*N,N,N′,N′*-tetramethyl-ethylenediamine) for another 15 min. After being washed with distilled water, the gel was illuminated with 400 μmol m^{-2} s^{-1} to initiate the photochemical reaction. The SOD activity was verified by KCN or H_2O_2 treatment (Pan et al. 1999).

The unit of SOD activity was defined as the amount of enzyme that inhibited the nitroblue tetrazolium photoreduction by 50% (Beauchamp and Fridovich 1971). SOD activity values are given in units per mg of protein. The results of three biological replicates were used for statistical analysis.

RNA isolation, cDNA synthesis, reverse transcription-PCR and cDNA cloning

Total RNA was isolated from the fertilized ovules with a TRIzol Reagent Kit (Invitrogen, Carlsbad, CA) according to the manufacturer's protocol. cDNA synthesis was performed with cDNA Reverse Transcription Kits (Applied Biosystems). The coding region of SODs was amplified with the primers presented in Supplementary Table S1. The PCR program was the following: 95 °C for 5 min and 40 × (95 °C for 20 s, 60 °C for 10 s, 72 °C for 30 s); and final elongation 72 °C for 7 min. All the amplicons were gel-purified, ligated into the pTZ57R/T cloning vector (Thermo FisherScientific) and cloned in XL1-Blue *E. coli* cells. Positively screened clones were sequenced on an ABI PRISM 3700 DNA Analyzer (Applied Biosystems).

Expression analysis by quantitative real-time PCR (qRT-PCR)

qRT-PCR was performed with the StepOnePLUS™ Real-Time system (Applied Biosystems) and SYBR Green Reagents (Applied Biosystems). Samples contained 10 µL of 2 × SYBR Green Master Mix, 0.4 µL each of forward and reverse primers of 10 µM of concentration, and 1 µL of synthesized cDNA to make the final reaction volume of 20 µL. We used the X. sorbifolium Actin-β gene for the internal control and normalization to calculate fold changes in gene expression of five *SOD* genes and one *SOD* copper chaperone gene. The relative expression levels of all samples were carried out in three biological replicates. All gene-specific primers used for qRT-PCR are presented in Supplementary Table S1.

Genomic amplification of the *XsSOD* genes

Genomic sequences of *XsCSD1, XsFSD1* and *XsMSD* were generated from the DNA template using PCR with forward and reverse primers presented in Supplementary Table S1, designed from their mRNA sequences. The PCR product was directly sequenced. The 5′-flanking sequences of *XsFSD1* and *XsMSD* genes were amplified by TAIL-PCR with the GenomeWalker™ Kit (TaKaRa). The gene-specific primers XsMSD-GW-R1, XsMSD-GW-R2 and XsMSD-GW-R3 (Supplementary Table S1) were designed on the basis of the above *SOD* genomic sequences. The PCR products were separated by 1.2% agarose gel electrophoresis. The purified DNA fragments were cloned into the pMD18-T vector (TaKaRa) and sequenced.

Sequence analysis

Amino acid sequences of the *XsSOD* genes were deduced and analyzed with the ExPASy Protparam tool (Wilkins et al. 1999). The BLAST program (http://www.ncbi.nlm.nih.gov) was used to search for homologues of the *SOD* genes from other plants. Multiple alignments were carried out with the ClustalW program (http://www.ebi.ac.uk/clustalw/). Phylogenetic analysis was performed according to the neighbor-joining method (Saitou and Nei 1987) using MEGA 5.02 (Kumar et al. 2004) with 1000 bootstrap replicates. An analysis for transcription response elements was carried out using the PlantCARE database (Lescot et al. 2002).

VIGS assays

A 350 bp fragment of *XsMSD* cDNA was amplified using the primers presented in Supplementary Table S1. The purified PCR products were digested with *EcoRI* and *KpnI* and ligated to pTRV2, resulting in the plasmid pTRV2-*XsMSD*. The plasmids were sequenced to verify correct insertion of the fragment and were then transformed into *Agrobacterium tumefaciens* GV3101. The cultures containing pTRV1 and pTRV2/pTRV2-*XsMSD* constructions were mixed in a 1:1 ratio, and then 1 mL of culture was injected into the base of the inflorescence axial 2 d after cross-pollination. Three independent biological replicates were performed for each treatment.

To monitor the expression of the *XsMSD* transcript in the pTRV2-*XsMSD*-inoculated fruits, total RNA of the pollinated ovules of the *XsMSD*-VIGS and pTRV2-empty inflorescences was extracted using an RNeasy Plant Mini Kit (Qiagen, Hilden, Germany). cDNA synthesis was conducted as described above with 250 ng of total RNA. qRT-PCR was performed with cDNA corresponding to 10 ng of total RNA in a 20 µL of reaction volume. The reaction mixture was prepared using SYBR Green Reagents (Applied Biosystems) and loaded into a StepOnePLUS™ Real-Time system (Applied Biosystems, Foster City, CA, USA). Three replications for each sample were used in the real-time analyses. Relative expression was determined by normalization against the *X. sorbifolium Actin-β* gene. The primers are presented in Supplementary Table S1.

Statistical analysis

Statistical analyses were conducted using the SPSS 16.0 software package (SPSS Inc, Chicago, IL, USA). Differences between the means were considered statistically significant difference at $P < 0.05$.

Results

Cytology of development of the fertilized ovules in *X. sorbifolium*

After fertilization, the amphitropous ovule of *X. sorbifolium* contains a long, curved embryo sac that is embedded within the massive nucellar tissue (Fig. 1a). The outer integument between the micropyle and chalaza at the raphal side becomes thickened by local periclinal and anticlinal divisions at the early stage of embryo sac development. Repeated divisions result in the formation of a radially stretched bulge that extends towards the embryo sac (Fig. 1a). The ovule grows rapidly after 8 DAP, and a considerable part of the volume of the ovule is taken up by the formation and enlargement of a liquid-filled vesicle at the chalazal end of the embryo sac. The inner cells of the nucellus that border the embryo sac rapidly undergo breakdown after 12 DAP (Fig. 1b). Several files of richly protoplasmic nucellar cells (hypostase) converge upon the chalazal tip of the embryo

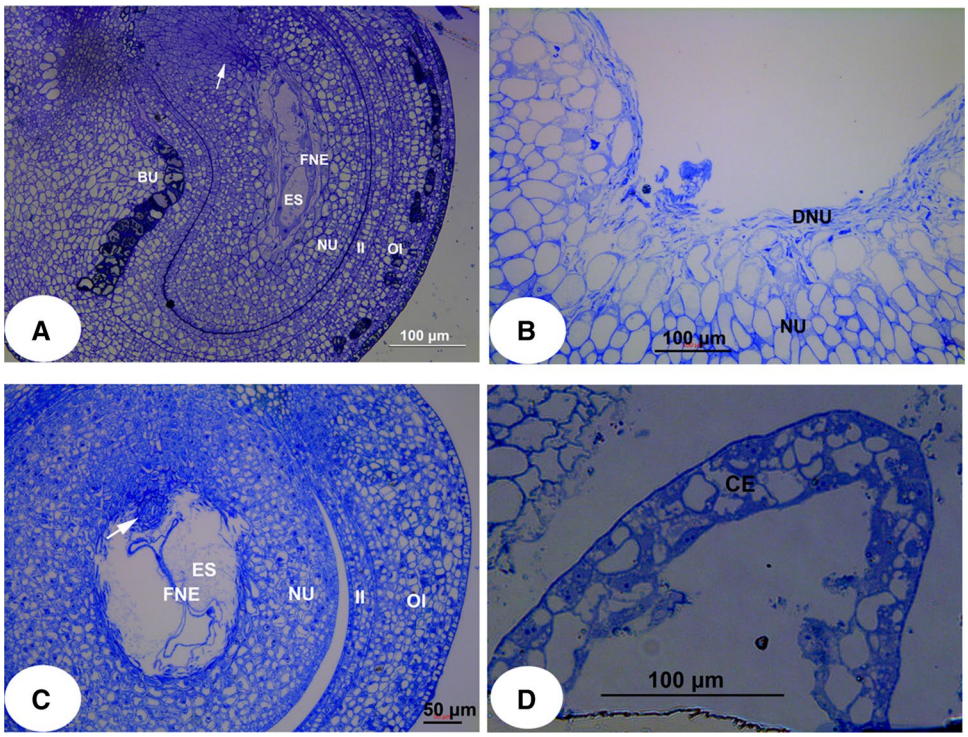

Fig. 1 The ovules of various developmental stages after fertilization in *Xanthoceras sorbifolium*. **a** A portion of the ovule at 4 days after cross-pollination, showing that a radially stretched bulge derived from the outer integument which extends into the embryo sac. **b** A portion of the ovule at 14 days after cross-pollination, showing that the inner cells of the nucellus rapidly disintegrate. **c** A portion of the ovule at 8 days after cross-pollination, showing that a global nucellar tissue delayed disintegrate. **d** A portion of the ovule at 20 days after cross-pollination, showing cellular endosperm at the micropylar end of the embryo sac. *BU* bulge, *CE* cellular endosperm, *DNU* degenerated nucellus, *ES* embryo sac, *FNE* free nuclear endosperm, *II* inner integument, *OI* outer integument

sac, suggesting a main route by which the vesicle may be nourished (Fig. 1a). These cells form a global appearance when other nucellar cells adjacent to the embryo sac disintegrated (Fig. 1c).

A few endosperm-free nuclei occur in the embryo sac within 48 h after pollination. Endosperm-free nuclei rapidly divide from 3 DAP to 13 DAP (Fig. 1a, c). With active mitosis, several hundred endosperm-free nuclei are produced and they become more or less evenly dispersed in a thin layer of cytoplasm around the periphery of the embryo sac. The cellular endosperm is observed at the micropylar part of the embryo sac at the early stage of global embryo 17 DAP (Fig. 1d). In the vesicle of the chalazal end of the embryo sac, no endosperm cell wall formation takes place.

SOD activity in the fertilized ovules of *X. sorbifolium*

Our nondenaturing PAGE enzyme assays identified three SOD activities in the fertilized ovules of *X. sorbifolium* (Fig. 2). The identities of the SOD activity bands were tested by preincubating the gels with well-characterized SOD inhibitors: KCN and H_2O_2. The results suggest that the band with the slowest mobility is MnSOD, the second band is FeSOD, and the fastest band is CuZnSOD. Three SOD isozyme activities were detected in all samples tested.

SOD activity staining in the gel indicated that FeSOD appeared as the dominant band and its activity exceeded that of MnSOD and CuZnSOD at various stages of development of the fertilized ovules (Fig. 2a). MnSOD, FeSOD and CuZnSOD activity displayed the highest level in the ovules at 18, 10 and 24 DAP, respectively (Fig. 3). The level of MnSOD activity remained relatively constant in the different stages of ovule development. The CuZnSOD activity level increased 2.6-fold from 3 to 24 DAP (Fig. 3a). The activity level of FeSOD and CuZnSOD markedly changed at the early stages of development of the fertilized ovules (Fig. 3a, b).

Organization of *X. sorbifolium SOD* genes

From the transcriptomic sequencing database of the fertilized ovules in *X. sorbifolium* (Zhou and Zheng 2015), we identified five putative *SOD* gene sequences, including two *CuZnSOD*, two *FeSOD*, one *MnSOD* and one *CCS* (copper chaperone for SOD). These sequences were named *XsCSD1, XsCSD2, XsFSD1, XsFSD2, XsMSD* and *XsCCS* (accession numbers MG322607, MG322609, MG322611, MG322613, MG322616, and MG322605, respectively). The phylogenetic analysis indicates that the *SOD* genes could be grouped into two clearly defined clades, based on function and location. CuZnSODs belong to the first clade and MnSOD and FeSODs are grouped into the second clade. XsCCS and AtCCS form a subgroup belonging to the first clade (Fig. 4).

The cDNA of *XsCSD1* is 1218 bp long with an open-reading frame (ORF) of 459 bp encoding a protein of 152 amino acids (Fig. S1A). We used mRNA from the fertilized ovules of *X. sorbifolium* to perform RT-PCR amplifications.

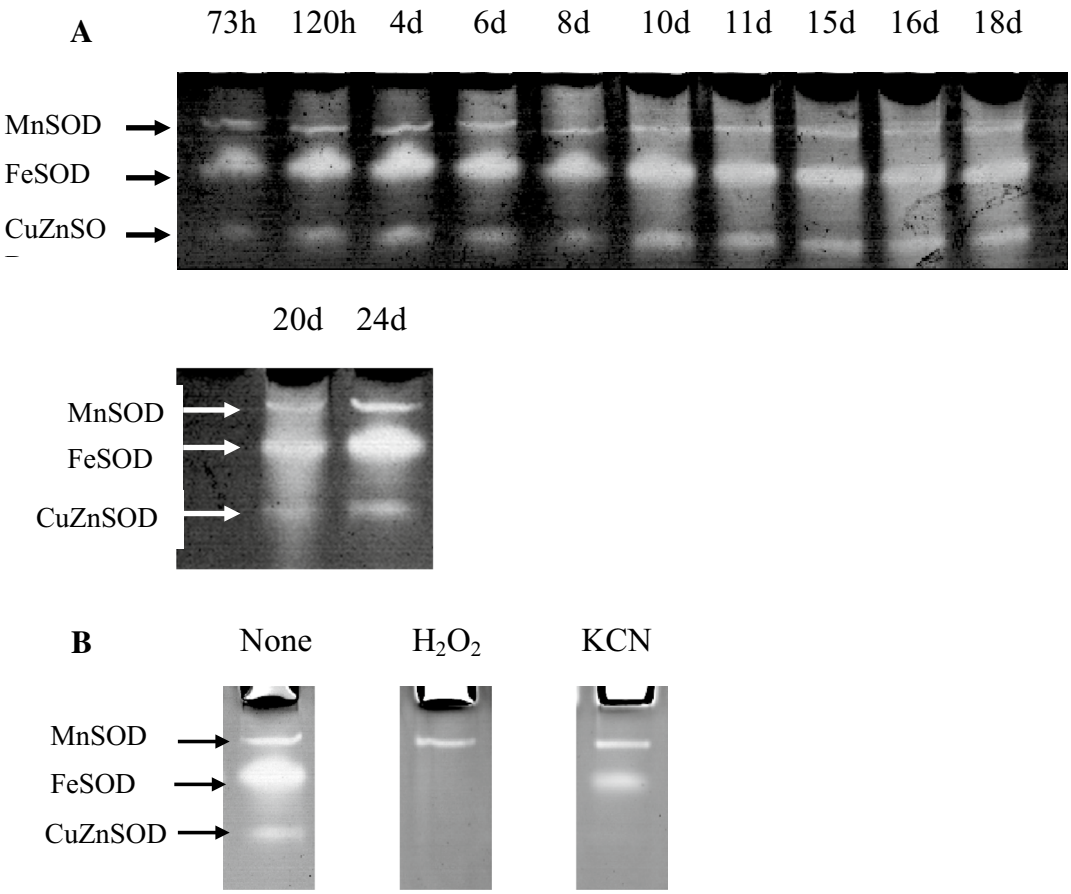

Fig. 2 Superoxide dismutase activity profile of the fertilized ovules of various developmental stages. **a** Crude proteins from the fertilized ovules were analysed on a nondenaturing PAGE gel and stained for SOD activity (clear gel regions). **b** Gels were preincubated with KCN (which inhibits CuZnSOD) or H_2O_2 (which inhibits both CuZnSOD and FeSOD) to facilitate identification of the different activities

The obtained amplicons were cloned and sequenced. The sequence (accession number MG322606) corresponded to the expected coding sequence of *XsCSD1*. The XsCSD1 contained two CuZnSOD family signature motifs (G^{115}FHLHEYGDTT^{125} and G^{209}NAGGRLACGVV^{220}). All the amino acids involved in the coordination of the copper (His-117, His-119, His-134 and His-191) and zinc (His-134, His-142, His-151 and Asp-154) were very well conserved in the reported CuZnSOD sequences, as were the two cysteines (Cys-128 and Cys-217) that were involved in a single disulfide bond (Fig. S2A). An N-terminal chloroplastic transit peptide sequence was predicted by ChloroP (http://www.cbs.dtu.dk/services/ChloroP) and TargetP (http://www.cbs.dtu.dk/services/TargetP), which indicates that XsCSD1 probably locates in the chloroplast. Phylogenetic analysis also indicates that XsCSD1 and other known or proposed plastid-targeted CuZnSODs are grouped into a clade (Fig. S3).

The *XsCSD2* cDNA is 1556 bp long and contains a 456-bp ORF encoding a 151 amino acids hypothetical protein that contains all of the conserved amino acids required for CuZnSOD activity (Fig. S1B). No signal peptide sequences were predicted by the ChloroP and the TargetP, indicating that the XsCSD2 probably locates in the cytoplasm (Fig. S2B). Phylogenetic analysis also indicated that the XsCSD2 clusters with the cytosolic CuZnSOD clade (Fig. S3), suggesting that it is cytosolic.

The *XsFSD1* cDNA contained a 933-nucleotide ORF encoding a predicted 310-amino acid protein with an amino-terminal chloroplastic transit peptide of 40 amino acids (Fig. S1C). The amplicons obtained by RT-PCR were cloned and sequenced. The sequence (accession number MG322610) agreed with the expected coding sequence of *XsFSD1*. The XsFSD1 had three FeSOD family signature motifs (F^{121}NNAAQAWNH^{130}, F^{175}GSGWAWLC^{183}, and D^{229}VWEHAYY^{236}), and four putative metal-binding sites for iron (His-78, His-130, Asp-229 and His-233) that mediated its catalytic activity (Fig. S2C).

The *XsFSD2* cDNA has a 759-nucleotide ORF. The deduced protein sequence is 252-amino acids long and contains all of the conserved amino acids for a functional FeSOD protein (Fig. S1D). No signal peptide sequence was

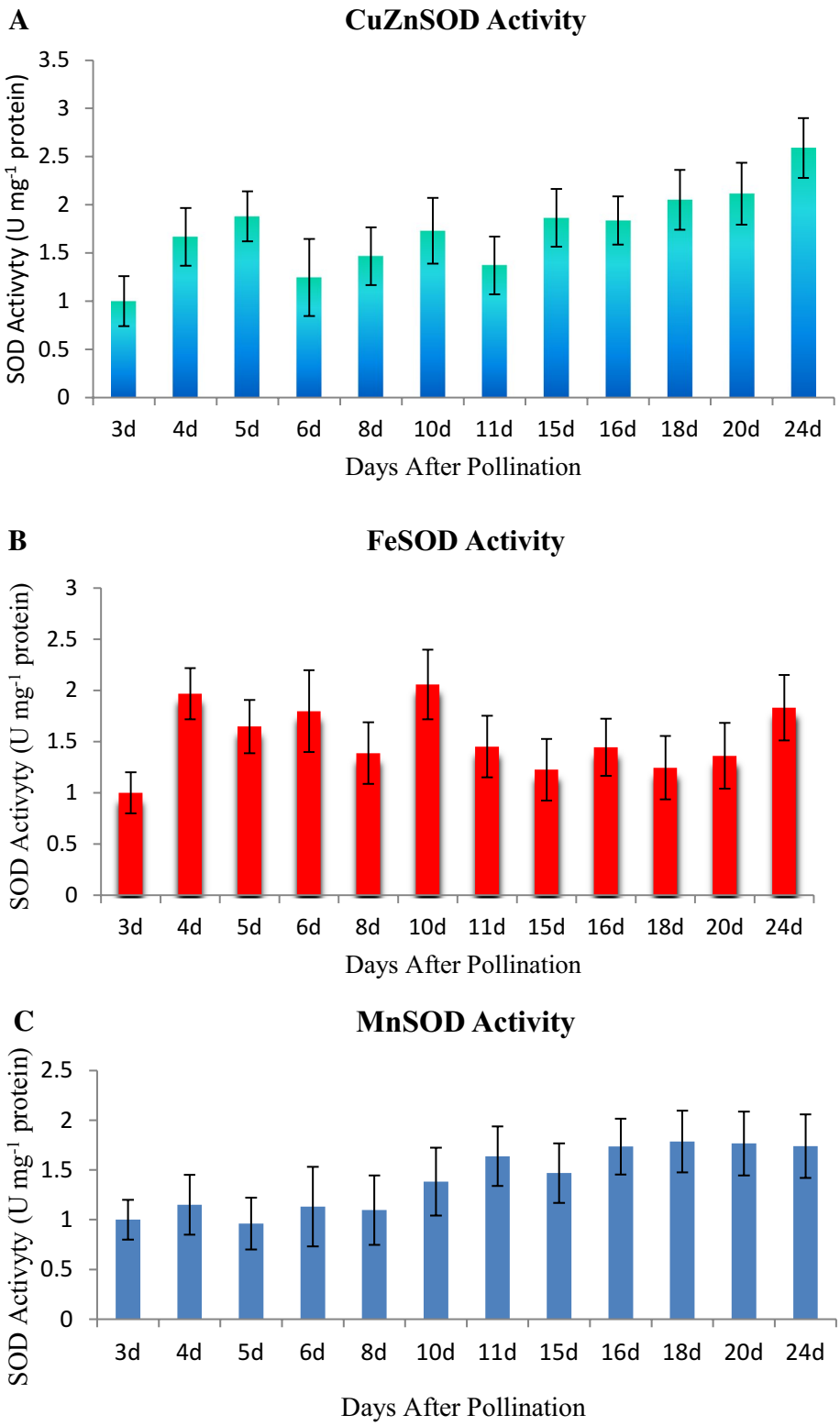

Fig. 3 The activity level of SOD isozymes changed at various developmental stages of the ovules after pollination in *Xanthoceras sorbifolioum*. The experiments were conducted with three independent biological replications. Values represent the means SD of three separate experiments

predicted, indicating that XsFSD2 is probably located in the cytoplasm (Fig. S2D).

The *XsMSD* cDNA is 1382 bp long and contains a 540-bp ORF encoding a hypothetical protein of 229 amino acids (Fig. S1E). The amplicons obtained by RT-PCR were cloned and sequenced. The sequence (Accession Number MG322614) corresponded to the expected coding sequence of *XsMSD*. The XsMSD possessed the characteristic

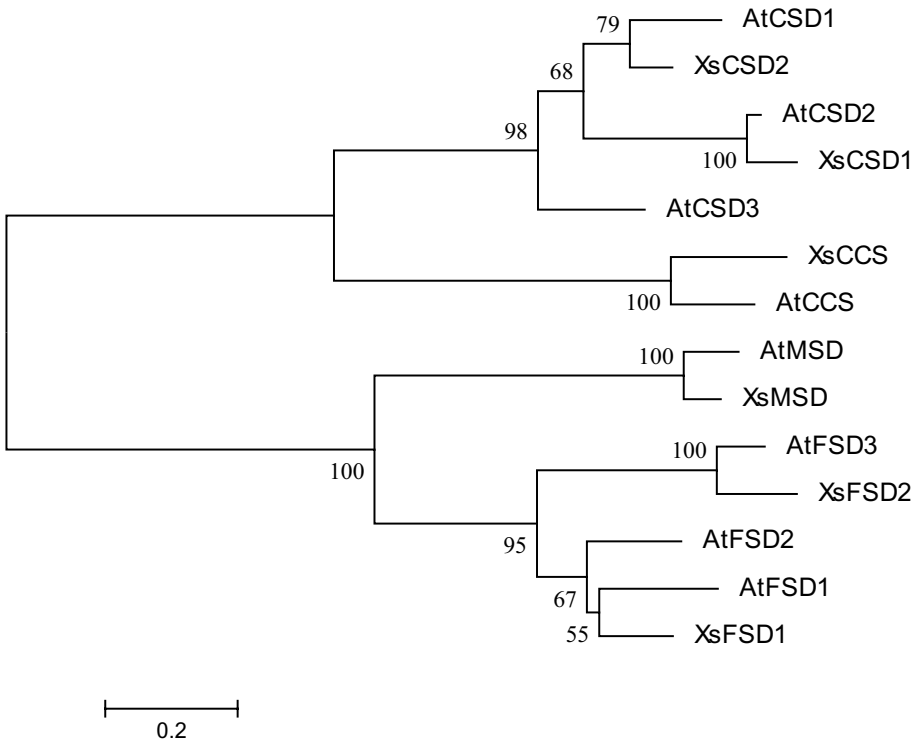

Fig. 4 Phylogenetic relationship among superoxide dismutase proteins in *Xanthoceras sorbifolium* and *Arabidopsis thaliana* was analyzed with Mega 5.1 using the neighbor-joining method. Numbers near branches represent Bootstrap support percentages. GenBank accession for each sequence represented in the tree are as follows: AtCSD1: NP172360; AtCSD2: NP565666; AtCSD3: NP197311; AtFSD1: NP197722; AtFSD2: NP199923; AtMSD: NP187703

Mn-SOD family signature ($D^{190}VWEHAYY^{197}$) and four clearly conserved residues coordinating Mn (His-53, His-101, Asp-190 and His-194) in the expected alignment positions (Fig. S2E). This protein contained an amino-terminal mitochondrial transit peptide with a potential cleavage site at amino acid position 25.

The full-length cDNA of *XsCCS* contains an open-reading frame (ORF) of 750 nucleotides (Fig. S1F). The deduced amino acid sequence shares 77% identity to that of $AtCCS_{cyt}$ (a cytosolic copper chaperone for SOD, CCS) in *A. thaliana*. Similar to AtCCScyt, XsCCS contains a N-terminal ATX1 domain in which there is a copper-binding consensus MXCXXC region found in the copper transporting ATPases and the cytosolic copper chaperones ATX1 (Fig. S4). The analyses suggest that the XsCCS may be a cytosolic copper chaperone for SOD.

Genomic structure and characterization of *XsSODs*

This study identified the genomic sequences of *XsCSD1, XsFSD1*, and *XsMSD* (accession numbers MG322608, MG322615, and MG322612, respectively) with lengths of 4060, 2587 and 3135 bp, respectively (Fig. 5). To investigate the numbers and positions of the exons and introns in these *XsSOD* genes, we compared each full-length cDNA sequence with their corresponding genomic DNA sequence. The *XsCSD*1 gene contains a 3952-bp segment spanning from the ATG translation start site to the stop codon. This gene consists of eight exons that were interrupted by seven introns (Fig. 5a). The coding sequence of the genomic gene matched with the corresponding cDNA sequence.

The *FSD*1 gene is comprised of nine exons separated by eight introns (Fig. 5b). The coding sequence of the genomic gene clearly matched with its cDNA counterpart. The *XsMSD* gene contains six exons and five introns (Fig. 5c), which is consistent with the *MnSOD* genes identified from other plant species (Fink and Scandalios 2002). The exons of *XsMSD* have identical or similar sizes to those of *MSD* genes from *Dimocarpus longan*, a member of the family Sapindaceae (Lin and Lai 2013), and *Brassica napus*. Exons 2 and 3 had the same length (47 and 126 bp, respectively) in the *MnSOD* genes of many plant species examined, such as *D. longan* (FJ590954.4), *Arabidopsis* (At3g10920), *Zea mays* (NC_024464.1), and *B. napus* (NW_013650564.1).

Promoters of *XsFSD1* and *XsMSD* genes

To investigate regulatory signals for *X. sorbifolium SOD* gene expression, the potential proximal promoter regions of *XsFSD1* and *XsMSD* were amplified and sequenced by the genome walking method. Transcription factor-binding motifs were predicted with the PlantCare database. The *XsFSD1* promoter is 1230 bp of the 5′-flanking region upstream from the ATG translation start site. Analysis of the 5′-flanking region of *XsFSD1* reveals six types of *cis*-acting regulatory elements involved in light responsiveness (Fig. S5A). Six hormone-responsive elements involved in responses to auxin (TGA-element), salicylic acid (TCA-element), methyl

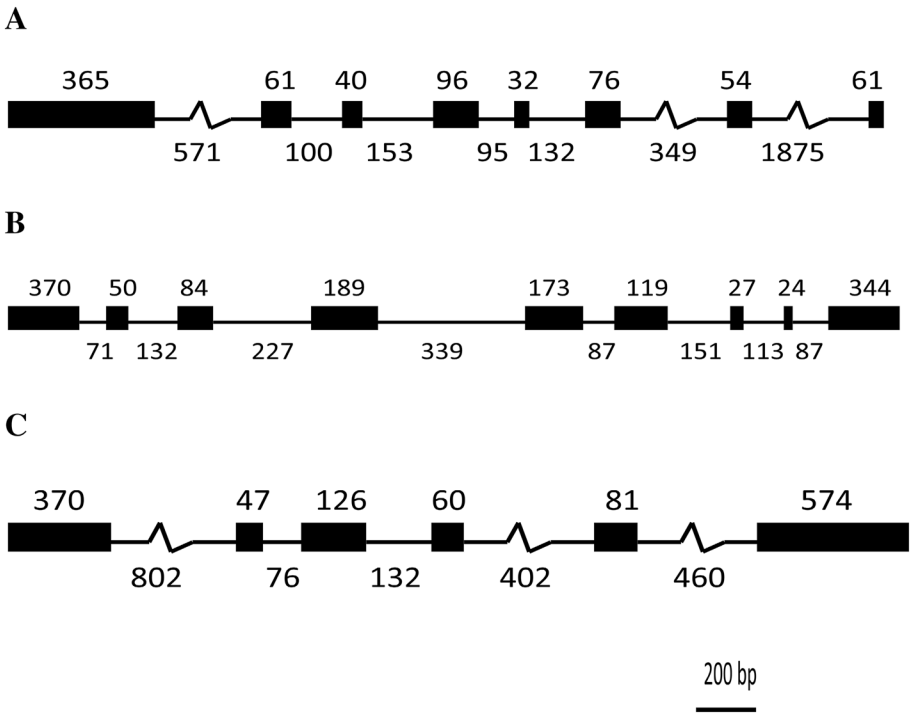

Fig. 5 Exon–intron organization of *XsSOD* genes in *Xanthoceras sorbifolium*. Exons are indicated by black boxes and introns are indicated by thin lines. All lengths are drawn to scale. Scale bar 200 bp. **a** *XsCSD1*; **b** *XsFSD1*; **c** *XsMSD*

jasmonate (CGTCA-motif), abscisic acid (ABRE) and gibberellins (GARE-motif and P-box) were identified in the *XsFSD1* proximal promoter region. We also found several stress-responsive regulatory elements including the anaerobic response element (ARE), MYB binding site involved in drought inducibility (MBS), heat shock element (HSE), and low-temperature stress responsiveness (LTR).

The investigation of the *XsMSD* promoter revealed a 995 bp segment of the 5′- flanking region upstream from the ATG translation start site. The PlantCare program also predicted many cis-acting regulatory elements in the 5′-flanking region of *XsMSD* (Fig. S5B), including light-responsive elements (Box II, G box, GAG motif, and Sp1), hormone-responsive elements involved in the abscisic acid responsiveness (ABRE) and in salicylic acid responsiveness (TCA-element), the antioxidant response element (ARE), HSEs, MBS, TC-rich repeats.

Expression profile of *XsSOD* genes in the fertilized ovules of *X. sorbifolium*

Quantitative RT-PCR analysis was used to determine the expression profile of 5 *SOD* genes (*XsCSD1, XsCSD2, XsFSD1, XsFSD2* and *XsMSD*) and a copper *SOD* chaperone gene along with developmental stages of *X. sorbifolium*-fertilized ovules. The six genes tested were widely expressed in the ovules of all the stages examined. Generally, the mRNA levels of each gene varied in the ovule of different stages. All the genes showed maximum expression in the ovules at 3 DAP (Fig. 6), a time point at which free nuclear endosperm rapidly develop and the majority of nucleus cells were conducting active division.

In the *XsCSD1* gene, mRNA levels were markedly decreased between 3 and 8 DAP (Fig. 6a). The low expression level of the *XsCSD1* gene was relatively constant from 21 to 29 DAP, a period in which the cellular endosperm and young embryo developed. The expression profile of *XsCSD2* is somewhat similar to that of *XsCSD1*. The *XsCSD2* mRNA level was significantly upregulated at 29 DAP compared with that of 21 DAP and 24 DAP (Fig. 6b).

The expression level of *XsFSD1* was very high in the early developmental stages before 8 DAP and decreased dramatically later (Fig. 6c). *XsFSD2* expression was conspicuously downregulated after it was highly expressed at 3 DAP (Fig. 6d).

XsMSD expression is slightly reduced at 6 DAP after high expression at 3 DAP (Fig. 6e). The *XsMSD* mRNA level markedly dropped at 8 DAP and then significantly increased again at 10 DAP. Thereafter, the level of *XsMSD* transcripts was dramatically reduced. The expression patterns of *XsCCS* were basically similar to those of *XsCSD1* from 6 to 29 DAP (Fig. 6f).

Reduced expression of *XsMSD* leads to abortion of the fertilized ovules

To examine the role of the *XsMSD* gene during development of fertilized ovules in *X. sorbifolium*, we conducted an experiment in which we inoculated inflorescences at 2 DAP with pTRV2-*XsMSD* plus pTRV1 plasmids aimed to silence

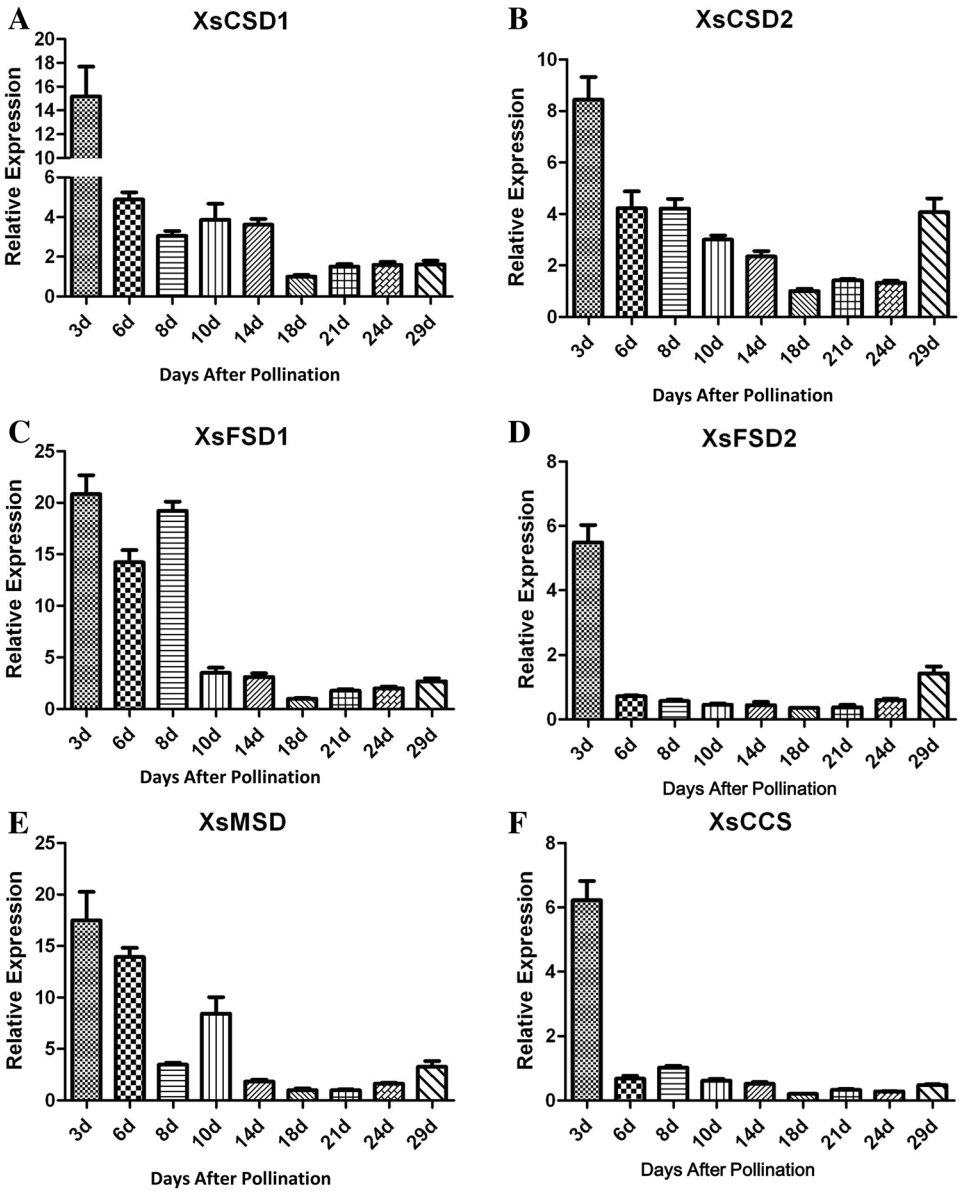

Fig. 6 Relative expression patterns of 5 *XsSOD* genes and 1 *XsCCS* gene by qRT-PCR analysis in the ovules sampled on various days after pollination in *Xanthoceras sorbifolium*. *XsActin-β* served as internal control and normalization of transcript level. The relative expression levels of all samples were carried out in three biological replicates. Error bars represent the standard deviation of the mean

the *XsMSD* gene. Of the inflorescences inoculated with pTRV2-*XsMSD* ($N = 50$), 42 aborted inflorescences were observed approximately 15 days after inoculation, suggesting successful silencing of *XsMSD* during the early stages of fruit development. No abnormal phenotypes were found in control inflorescences inoculated with pTRV2-empty plus pTRV1. pTRV2-*XsMSD*-inoculated inflorescences showed degenerated endosperm development in all the ovules examined ($N = 100$) (Fig. 7). Mock-treated (pTRV2-empty) inflorescences were nearly undistinguishable from untreated inflorescences with respect to the development of fertilized ovules, suggesting no visible viral effects in this plant at the ovule development level. RT-PCR analyses confirmed a downregulation of endogenous *XsMSD* mRNA levels in the ovules of pTRV2-*XsMSD* inflorescences compared to those of the mock-treated inflorescences (Fig. 8). To confirm that the reduced expression level of *XsMSD* transcripts in the pTRV2-*XsMSD* ovules was due to viral vectors, our RT-PCR analysis validated the presence of TRV1 and TRV2 transcripts in control ovules (inoculated with pTRV1 plus pTRV2-empty plasmids) and pTRV2-*XsMSD* ovules (inoculated with pTRV1 plus pTRV2-*XsMSD* plasmids; Fig. 9).

Discussion

Multiple *SOD* genes in *X. sorbifolium*

Plants contain multiple SOD isozymes. Many unique and highly compartmentalized SODs have been biochemically

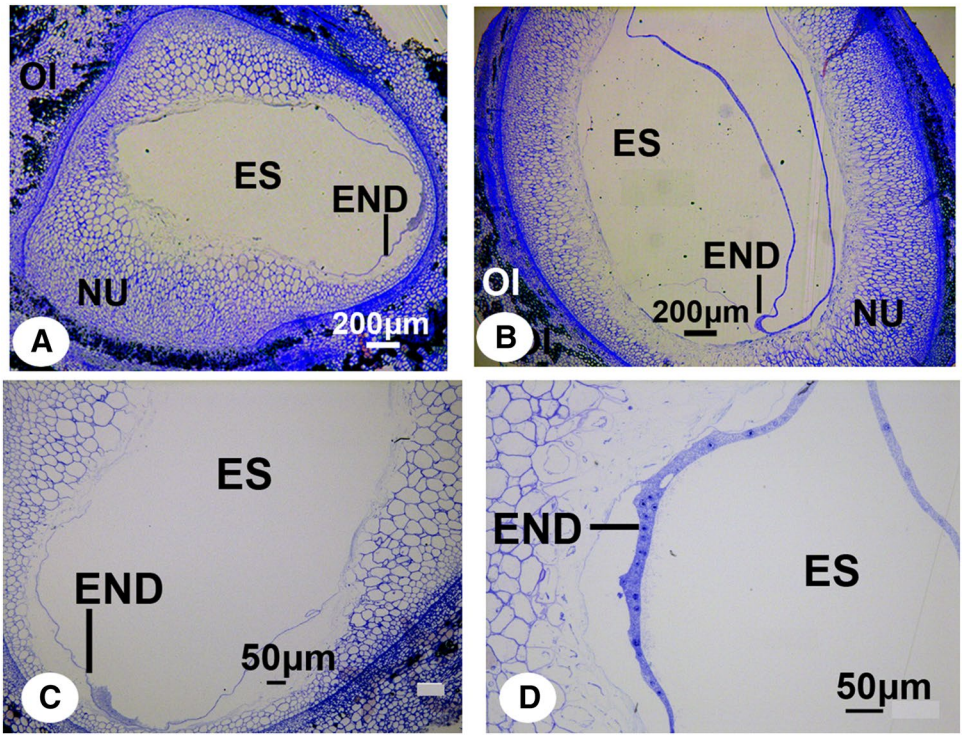

Fig. 7 Longitudinal sections of the fertilized ovules at 20 days after pollination. **a** Showing a degenerated ovule from a pTRV2-*XsMSD*-inoculated inflorescence. **b** Showing normally developing ovule from mock-treated (pTRV2-empty) inflorescence. **c** Showing degenerated free nuclear endosperm in the ovule of **a. d** Showing normal free nuclear endosperm in the ovule of **b**. *ES* embryo sac, *END* endosperm, *Nu* nucellus, *OI* outer integument

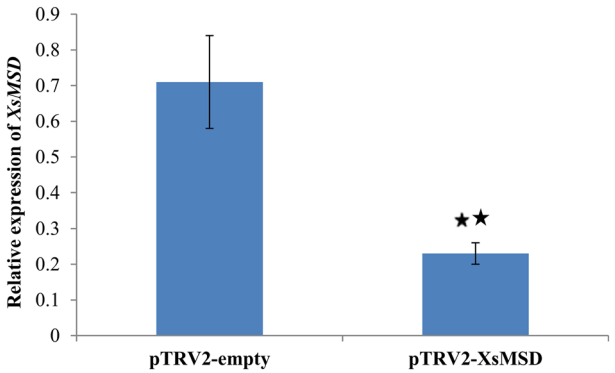

Fig. 8 RT-PCR detection of *XsMSD* transcripts in control ovules (inoculated with pTRV1 plus pTRV2-empty plasmids), and pTRV2-*XsMSD* ovules (inoculated with pTRV1 plus pTRV2-*XsMSD* plasmids). *XsActin-β* served as internal control and normalization of transcript level. The relative expression levels were carried out in three biological replicates. Asterisks indicate a significant difference compared with the control group at 99% confidence intervals after ANOVA

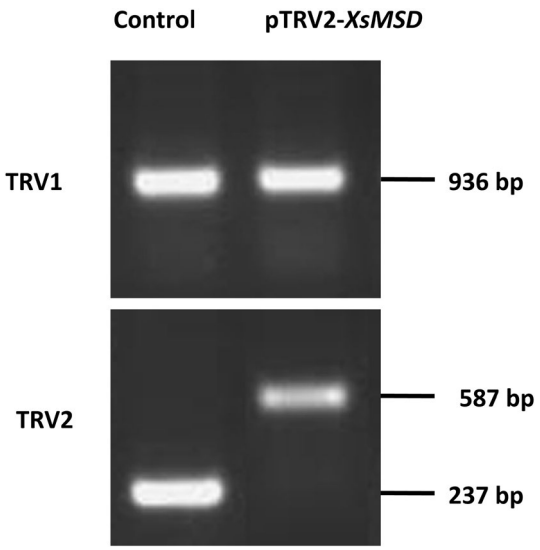

Fig. 9 RT-PCR detection of TRV1 and TRV2 viral transcripts in control ovules (infiltrated with pTRV1 and empty pTRV2 plasmids), and pTRV2-*XsMSD* ovules (infiltrated with pTRV1 and pTRV2-*XsMSD* plasmids)

and molecularly characterized in plants to date (Momcilovic et al. 2014). The present study identified three families of *SOD* genes (*CuZnSOD, FeSOD*, and *MnSOD*) in the fertilized ovules of *X. sorbifolium*. This plant expresses at least five *SOD* genes encoding proteins targeted to at least three subcellular compartments: chloroplasts, cytoplasm, and mitochondria. It is likely that each SOD protein may protect against a subset of oxidative stresses and that a variety of SODs are deployed to fully combat endogenous and environmental stresses.

In silico analysis indicated two isoforms of CuZnSODs (XsCSD1 and XsCSD2) localized in the cytosol and the chloroplasts in *X. sorbifolium*, respectively. There is no significant sequence identity between chloroplastic XsCSD1

and cytosolic XsCSD2 (61% identity, query cover = 65%, *E* value = 5e−66). They are differently compartmentalized; however, these two proteins may function similarly, but in different tissues and at different times.

FeSODs have initially been thought of as localized essentially in the plastid organelle within the plants or algae (Van Camp et al. 1990), but a non-chloroplastic FeSOD isozyme was later found to be localized in the mitochondria in wheat and in the nucleus of *Sesbania rostrata* in association with chromatin (Srivalli and Khanna-Chopra 2001). In legume nodules, an original group of FeSODs with cytosolic localization has been detected in soybean and cowpea plants (Moran et al. 2003). The present studies identified two isoforms of FeSODs with cytosolic and chloroplastic locations in *X. sorbifolium*, respectively. These two types of *XsFSDs* are expressed differentially in the fertilized ovules depending on the stage after pollination. Plastidic *XsFSD1* mRNA levels were significantly higher during 3 to 8 DAP than during 10 to 29 DAP, while cytosolic *XsFSD2* mRNA levels were significantly higher at 3 and 29 DAP compared with during 6 to 24 DAP.

A copper SOD chaperone gene in *X. sorbifolium*

Copper in the CuZnSOD protein plays a catalytic role in dismutation of superoxide to molecular oxygen and peroxide (Forman and Fridovich 1973). Intracellular copper trafficking is mediated by unique chaperones functioning to deliver this metal to copper-containing proteins. Lys7, ATX1, and COX17 were identified as copper chaperones in yeast (*Saccharomyces cerevisiae*), and they are responsible for copper incorporation into CuZnSOD (Glerum et al. 1996; Horecka et al. 1995; Lin et al. 1997).

The copper chaperone for SOD (CCS) in *Arabidopsis* contains three functionally distinct protein domains: ATX1-like domain, central domain, and C-terminal domain (Chu et al. 2005; Cohu et al. 2009). One *AtCCS* gene encodes both the cytosolic and chloroplastic forms of AtCCS and activates CuZnSOD activities at different subcellular locations (Chu et al. 2005; Huang et al. 2012). Similar to AtCCS, XsCCS also contains a central domain which is flanked by an ATX1-like domain and a C-terminal domain. The ATX1-like and the C-terminal domain contain a putative copper-binding motif MXCXXC and a CXC motif, respectively. In addition, the central domain shares 30% sequence identity with XsCSD2. These data suggested that the XsCCS in *X. sorbifolium* could have similar functions to the AtCCS in *Arabidopsis*. Our RT-PCR analysis indicated a high expression for the copper SOD chaperone gene at the early stage of the ovule development after pollination in *X. sorbifolium*, suggesting an important role in free nuclear endosperm development.

Expression of the *SOD* genes during development of the fertilized ovules in *X. sorbifolium*

The RT-PCR analysis in the fertilized ovules of *X. sorbifolium* indicated that all the *SOD* genes and the *XsCCS* gene showed the highest expression at 3 DAP, a time point in which free nuclear endosperm rapidly develop, and the majority of nucleus cells are conducting the most active division, suggesting that oxygen consumption and related metabolism were the highest and ROS formation was favored. The highest expression of *SODs* at this time point can scavenge the rapidly producing ROS and provides protection against oxidative stress. However, during cellular endosperm development (18–29 DAP), their mRNA levels decreased. It is likely that the *XsSOD* genes play a crucial role in redox regulation of cell proliferation at the early developmental stages of the fertilized ovules in *X. sorbifolium*.

Activity of the XsSOD isoenzymes in *X. sorbifolium*

Various XsSOD isoenzymes showed different activity levels at different developmental stages of the fertilized ovules in *X. sorbifolium*. During the exponential phase of endosperm-free nucleus mitosis at 10 DAP, XsFSD activity markedly increased. The activity of the XsMSD isoenzyme was relatively low in the early developmental stages of fertilized ovules, started to increase with age and reached the peak at 18 DAP, a time point in which cellular endosperm began to form, suggesting some possible roles in cellularization of free nuclear endosperm. The increase in XsMSD enzyme activity could be indicative of increased production of reactive oxygen species in mitochondria and a build-up of a protective mechanism to reduce oxidative damage triggered by rapid endosperm cell division and PCD in the nucellar tissue of ovules. Different SOD isoenzymes might play different roles in different ovule developmental stages. The fact that the SOD proteins do not mirror the pattern of *SOD* transcript expression suggests that there is a translational or posttranslational regulation of the SODs.

Genomic characterization of the *XsSOD* genes

The promoter regions of the *FSD* gene in *X. sorbifolium* and *D. longan* share some common features (Lin and Lai 2013). For example, the *FSD* genes in these two members of the Sapindaceae family contain hormone-responsive elements involved in response to methyl jasmonate (TGACG-motif), gibberellins (P-box), and stress-responsive regulatory elements such as MBS (MYB binding site involved in drought inducibility), a cis-acting regulatory element required for endosperm expression (Skn-1_motif). The functional importance of these sites is not clear at this time. Previous studies indicated that KUODA1 (KUA1), a MYB-like TF, functions

as a positive regulator of cell expansion during leaf development by altering apoplastic ROS homeostasis in *A. thaliana* (Lu et al. 2014). ROS homeostasis controls expansion of the cell and the final size of the organ. The MYB binding site in the 5′-flanking region of the *XsFSD1* gene suggested the possibility of regulation in ROS homeostasis during development of the fertilized ovules of *X. sorbifolium*.

The *XsMSD* promoter region contains typical CAAT and TATA boxes. They were also found in the promoter region of the *D. longan MnSOD* gene but were missing in the wheat *MnSOD*. The *MnSOD* is not only expressed constitutively but is also extremely responsive to a variety of endogenous and exogenous stress stimuli (Wang et al. 2004; Li et al. 2009). Intense light resulted in increased expression of maize *MnSOD* (White and Scandalios 1988). Five light-responsive elements (Box II, G-box, GAG-motif, Sp1 and chs-Unit 1 m1) were identified in the promoter region of the *XsMSD*. The *XsMSD* promoter region also contained many cis-acting regulatory elements, such as MBS, ARE, 5′UTR Py-rich stretch, and circadian, which are shared with that of the *D. longan MSD* and GCN4_motif, AAGAA-motif, and G-box, which are shared with that of the monocot wheat *MSD*. Such a high level of homology in the 5′-flanking sequence of the *MnSOD* genes suggests that intense evolutionary factors have preserved key regulatory regions for this gene.

TRV-based VIGS of the *XsMSD* resulted in fruit abortion

It is generally difficult to use a transgenic approach for the evaluation of gene function in fruit trees. Even if transgenic plants are obtained, it is impossible to evaluate sexual reproduction traits during a short time due to the long juvenile phase of the trees. This study tested the application of the TRV-based virus vector system in *X. sorbifolium* inflorescence, resulting in the transcriptional silencing of the *MSD* gene of the fertilized ovules within the flowers co-infiltrated with pTRV1 and pTRV2. The *XsMSD* gene silencing led to the arrest of fertilized ovule development and the abortion of the young fruits. This work provided direct evidence that the *MSD* gene is closely related to early development of the fertilized ovules and fruits in *X. sorbifolium*. Our results suggested the possible application of the VIGS system for functional studies of the genes related to seed development.

Conclusions

This work revealed different activity levels of various XsSOD isoenzymes at different developmental stages of the fertilized ovules in *X. sorbifolium*. Five *SOD* genes (*XsCSD1, XsCSD2, XsFSD1, XsFSD2* and *XsMSD*) and a copper *SOD* chaperone gene were widely expressed in the ovules of all the stages examined and their mRNA levels varied along with the developmental stages. The transcriptional silencing of the *XsMSD* gene resulted in the arrest of fertilized ovule development. The present data suggest for the first time that *SOD* genes might be closely associated with the fate of ovule development (aborted or viable) after fertilization in *X. sorbiforlium*.

Author contribution statement QZ conceived and designed the experiments; QZ performed the experiments; QZ and QC analyzed the data; QZ wrote the manuscript.

Acknowledgements We would like to thank Jie Wen and Fengqin Dong for technical help. This work was supported by the National Natural Science Foundation of China (30972344, 31370611 and 31570680) and Beijing Natural Science Foundation (6172028).

Compliance with ethical standards

Conflict of interest The authors declare that they have no conflict of interest.

References

Beauchamp C, Fridovich I (1971) Superoxide dismutase: improved assays and an assay applicable to acrylamide gel. Anal Biochem 44:276–287

Chu CC, Lee WC, Guo WY, Pan SM, Chen LJ, Li HM, Jinn TL (2005) A copper chaperone for superoxide dismutase that confers three types of copper/zinc superoxide dismutase activity in *Arabidopsis*. Plant Physiol 139:425–436. https://doi.org/10.1104/pp.105.065284

Cohu CM, Abdel-Ghany SE, Gogolin Reynolds KA, Onofrio AM, Bodecker JR, Kimbrel JA, Niyogi KK, Pilon M (2009) Copper delivery by the copper chaperone for chloroplast and cytosolic copper/zinc-superoxide dismutases: regulation and unexpected phenotypes in an *Arabidopsis* mutant. Mol Plant 2:1336–1350. https://doi.org/10.1093/mp/ssp084

Fink RC, Scandalios JG (2002) Molecular evolution and structure–function relationships of the superoxide dismutase gene families in angiosperms and their relationship to other eukaryotic and prokaryotic superoxide dismutases. Arch Biochem Biophys 399:19–36

Forman HJ, Fridovich I (1973) On the stability of bovine superoxide dismutase: the effects of metals. J Biol Chem 248:2645–2649

Glerum DM, Shtanko A, Tzagoloff A (1996) Characterization of COX17, a yeast gene involved in copper metabolism and assembly of cytochrome oxidase. J Biol Chem 271:14504–14509

Gupta DK, Pena LB, Romero-Puertas MC, Hernández A, Inouhe M, Sandalio LM (2017) NADPH oxidases differentially regulate ROS metabolism and nutrient uptake under cadmium toxicity. Plant Cell Environ 40:509–526

Horecka J, Kinsey PT, Sprague GFJ (1995) Cloning and characterization of the *Saccharomyces cerevisiae* LYS7 gene: evidence for function outside of lysine biosynthesis. Gene 162:7–92

Huang CH, Kuo WY, Weiss C, Jinn TL (2012) Copper chaperone-dependent and -independent activation of three copper–zinc superoxide dismutase homologs localized in different cellular

compartments in *Arabidopsis*. Plant Physiol 158:737–746. https://doi.org/10.1104/pp.111.190223

Kliebenstein DJ, Monde RA, Last RL (1998) Superoxide dismutase in *Arabidopsis*: an eclectic enzyme family with disparate regulation and protein localization. Plant Physiol 118:637–650

Kumar S, Tamura K, Nei M (2004) MEGA3: integrated software for molecular evolutionary genetics analysis and sequence alignment. Brief Bioinform 5:150–163. https://doi.org/10.1093/bib/5.2.150

Lescot M, Dehais P, Thijs G, Marchal K, Moreau Y, Van de Peer Y, Rouze P, Rombauts S (2002) PlantCARE, a database of plant *cis*-acting regulatory elements and a portal to tools for in silico analysis of promoter sequences. Nucleic Acids Res 30:325–327. https://doi.org/10.1093/nar/30.1.325

Li W, Qi L, Lin X, Chen H, Ma Z, Wu K, Huang S (2009) The expression of manganese superoxide dismutase gene from *Nelumbo nucifera* responds strongly to chilling and oxidative stresses. J Integr Plant Biol 51:279–286. https://doi.org/10.1111/j.1744-7909.2008.00790.x

Lin YL, Lai ZX (2013) Superoxide dismutase multigene family in longan somatic embryos: a comparison of CuZn-SOD, Fe-SOD, and Mn-SOD gene structure, splicing, phylogeny, and expression. Mol Breed 32:595–615. https://doi.org/10.1007/s11032-013-9892-2

Lin SJ, Pufahl RA, Dancis A, O'Halloran TV, Culotta VC (1997) A role for the *Saccharomyces cerevisiae* ATX1 gene in copper trafficking and iron transport. J Biol Chem 272:9215–9220

Lu D, Wang T, Persson S, Mueller-Roeber B, Schippers JHM (2014) Transcriptional control of ROS homeostasis by KUODA1 regulates cell expansion during leaf development. Nat Commun 5:3767. https://doi.org/10.1038/ncomms4767

María VM, Diego FF, Venkatesan S, Eduardo JZ, Gabriela CP (2013) *Oiwa*, a female gametophytic mutant impaired in a mitochondrial manganese-superoxide dismutase, reveals crucial roles for reactive oxygen species during embryo sac development and fertilization in *Arabidopsis*. Plant Cell 25:1573–1591. https://doi.org/10.1105/tpc.113.109306

McCord JM, Fridovich I (1988) Superoxide dismutase: the first twenty years (1968–1988). Free Radic Biol Med 5:363–369

Mittler R, Vanderauwera S, Suzuki N, Miller G, Tognetti VB, Vandepoele K et al (2011) ROS signaling: the new wave? Trends Plant Sci 16:300–309. https://doi.org/10.1016/j.tplants.2011.03.007

Momcilovic I, Pantelic D, Hfidan M, Savic J, Vinterhalter D (2014) Improved procedure for detection of superoxide dismutase isoforms in potato, *Solanum tuberosum* L. Acta Physiol Plant 36:2059–2066. https://doi.org/10.1007/s11738-014-1583-z

Moran JF, James EK, Rubio MC, Sarath G, Klucas RV, Becana M (2003) Functional characterization and expression of a cytosolic iron-superoxide dismutase from cowpea root nodules. Plant Physiol 133:773–782. https://doi.org/10.1104/pp.103.023010

Pan SM, Hwang GB, Liu HC (1999) Over-expression and characterization of copper/zinc-superoxide dismutase from rice in *Escherichia coli*. Bot Bull Acad Sin (Taipei) 40:275–281

Saitou N, Nei M (1987) The neighbor-joining method: a new method for reconstructing phylogenetic trees. Mol Biol Evol 4:406–425

Sandalio LM, Rodríguez-Serrano M, Romero-Puertas MC, del Rio LA (2013) Role of peroxisomes as a source of reactive oxygen species (ROS) signalling molecules. Subcell Biochem 69:231–255. https://doi.org/10.1007/978-94-007-6889-5_13

Singh R, Singh S, Parihar P, Mishra RK, Tripathi DK, Singh VP, Chauhan DK, Prasad SM (2016) Reactive oxygen species (ROS): beneficial companions of plants' developmental processes. Front Plant Sci 7:1299. https://doi.org/10.3389/fpls.2016.01299

Spurr AR (1969) A low viscosity epoxy resin embedding medium for electron microscopy. J Ultrastruct Res 26:31–43

Srivalli B, Khanna-Chopra R (2001) Induction of new isoforms of superoxide dismutase and catalase enzymes in the flag leaf of wheat during monocarpic senescence. Biochem Biophys Res Commun 288:1037–1042. https://doi.org/10.1006/bbrc.2001.5843

Suzuki N, Koussevitzky S, Mittler R, Miller G (2012) ROS and redox signalling in the response of plants to abiotic stress. Plant Cell Environ 35:259–270. https://doi.org/10.1111/j.1365-3040.2011.02336.x

Tsukagoshi H, Busch W, Benfey PN (2010) Transcriptional regulation of ROS controls transition from proliferation to differentiation in the root. Cell 143:606–616. https://doi.org/10.1016/j.cell.2010.10.020

Van Camp W, Bowler C, Villarroel R, Tsang EWT, Van Montagu M, Inze D (1990) Characterization of iron superoxide dismutase cDNAs from plants obtained by genetic complementation in Escherichia coli. Proc Natl Acad Sci USA 87:9903–9907

Wang Y, Ying Y, Chen J, Wang X (2004) Transgenic Ar*abidopsis* overexpressing Mn-SOD enhanced salt-tolerance. Plant Sci 167:671–677. https://doi.org/10.1016/j.plantsci.2004.03.032

White JA, Scandalios G (1988) Isolation and characterization of a cDNA for mitochondrial manganese superoxide dismutase (SOD-3) of maize and its relation to other manganese superoxide dismutase. Biochem Biophys Acta 951:61–70

Wilkins MR, Gasteiger E, Bairoch A, Sanchez JC, Williams KL, Appel RD, Hochstrasser DF (1999) Protein identification and analysis tools in the ExPASy server. Methods Mol Biol 112:531–552

Zhou QY, Liu GS (2012) The embryology of *Xanthoceras* and its phylogenetic implications. Plant Syst Evol 298:457–468. https://doi.org/10.1007/s00606-011-0558-4

Zhou QY, Zheng YR (2015) Comparative de novo transcriptome analysis of fertilized ovules in *Xanthoceras sorbifolium* uncovered a pool of genes expressed specifically or preferentially in the selfed ovule that are potentially involved in late-acting self-incompatibility. PLOS One 10:e0140507. https://doi.org/10.1371/journal.pone.0140507

Zhou QY, Zheng YR, Lai LM, Du H (2017) Observations on sexual reproduction in *Xanthoceras sorbifolium* (Sapindaceae). Acta Bot Occident Sin 37:0014–0022. https://doi.org/10.7606/j.issn.1000-4025.2017.01.0014